Reports

Simulated Wind Pollination and Airflow Around Ovules of Some Early Seed Plants

Abstract. *Scale models of various early seed plant ovules and cupules were analyzed both for their characteristic air disturbance patterns and for the frequency of impact with airborne models of pollen (pseudopollen). The fossils on which the models were based had been arranged in an evolutionary sequence purporting to show the origin of the integument by the acropetal fusion and reduction in length of a subtending truss of lobes. Wind tunnel analyses of scale models showing the various stages in the consolidation of these preintegumentary lobes indicated that turbulent flow increases and becomes localized around the nucellar apex (salpinx) with the syngenesis and length reduction of those lobes. Similarly, the frequency of windborne pseudopollen impact increased. Thus, the transition from the megasporangium to the fully integumented ovule appears to favor increased wind-mediated pollination.*

Studies of early seed plant fossils indicate that the transition from the megasporangium (nucellus) to the integumented ovule (immature seed) involved at least two evolutionary trends (*1*): (i) the modification of the nucellar apex into a pollen reception site (salpinx or lagenostome) and (ii) the formation of an integument, possibly by the progressive acropetal fusion and reduction in length of a sterile truss of lobes (preintegumentary lobes) that subtended the nucellus. A similar pattern of acropetal fusion and reduction of modified branches is thought to have produced the ensheathing of seeds in secondary structures termed cupules (*1*). The functional significance of cupulate ovules is unclear; however, some investigators believe that they were analogous to carpels (*1*). Both trends are apparently interrelated since the complexity and size of the salpinx decreased as the preintegumentary lobes consolidated into an integument with a distal micropyle. Various reasons for these trends may be proposed (*2*), including selective pressures for protection and pollination. The likelihood that the earliest seed plants were wind-pollinated is a basis for inferring a reproductive strategy for the modification of sterile lobes about the nucellus, provided that such modifications could be shown to increase the probability of pollination. Similarly, inferences based on the insect fossil record (*3*) suggest that predation may have selected for the protection of the megagametophyte by a mechanical barrier or a substitute food source. In this report evidence is presented to partially support the supposition that the evolutionary trends seen in some early seed plant ovules were important in facilitating windborne pollen capture by the salpinx and later the micropyle. Detailed analyses of airflow disturbance patterns around models of ovules and cupules scaled to known fossils provide information on airstream patterns and their influence on the probability of wind pollination. It must be noted that fossil taxa studied are thought to represent the generalized stages of ovule evolution rather than to comprise an actual phyletic line.

For the purposes of illustration, models of *Genomosperma kidstoni* (Fig. 1, A and B), *G. latens* (Fig. 1, C and D), *Eurystoma angulare* (Fig. 1, E and F, I and J), and *Stamnostoma huttonense* (Fig. 1,

Table 1. Wind tunnel parameters and pseudopollen to model surface impact scores.

Genus	Length (cm)		Flow rate (cm/sec)	Impact number (400 maximum)	Preintegumentary lobes (PL)		Pseudopollen impact on megasporangium		Distal PL + NA (%)
	Model	Fossil			Proximal (%)	Distal (%)	Proximal (%)	Distal (NA) (%)	
Ovule									
Genomosperma kidstoni									
Parallel	16	1.6	45	59	25.2 (9.2)*	20.3 (6.0)	20.6 (3.7)	33.9 (4.2)	54.2
Tangential	16	1.6	45	32	12.5 (7.1)	36.5 (3.9)	21.0 (1.1)	30.0 (3.5)	66.5
Genomosperma latens									
Parallel	8	0.8	45	117	12.1 (6.4)	33.5 (5.7)	12.1 (3.7)	37.2 (7.6)	70.7
Tangential	8	0.8	45	110	21.2 (8.1)	28.1 (5.3)	24.0 (7.7)	25.7 (5.6)	53.8
Eurystoma angulare									
Parallel	8	0.8	45	173	12.7 (4.4)	45.2 (10.3)		42.0 (11.7)	87.2
Tangential	8	0.8	45	152	18.4 (9.0)	37.3 (11.1)		44.3 (10.3)	81.6
Stamnostoma huttonense									
Parallel	8	0.37	14	110	20.2 (6.6)	39.7 (8.0)		40.1 (9.4)	79.8
Tangential	8	0.37	14	92	23.0 (5.9)	34.0 (9.6)		43.0 (8.9)	77.0
							Ovule		
Cupule					Cupule axes		PL	NA	
Eurystoma angulare									
Parallel	14 (8)†	≅ 1.4 (0.8)	45	246 (100)†	40.2 (12.6)		32.1 (10.9)	27.7 (9.2)	59.8
Tangential	14 (8)	≅ 1.4 (0.8)	45	211 (102)	33.1 (8.0)		30.0 (10.1)	36.9 (5.2)	66.9
Stamnostoma huttonense									
Parallel	18 (8)	≅ 1.8 (0.8)	14	241 (77)	22.5 (13.1)		32.9 (8.3)	44.6 (12.2)	77.5
Tangential	18 (8)	≅ 1.8 (0.8)	14	198 (98)	21.2 (10.8)		30.8 (7.0)	48.0 (13.0)	78.8

*Equal to $N_p/N_t \times 100$ percent, where N_p is the number of pollen analogs per unit area N, and N_t is the total number of pollen analogs on the model's surface. Standard deviation (in parentheses) is based on ten trials. †Cupule (ovule).

0036-8075/81/0116-0275$00.50/0

G, H, and K) were constructed. *Genomosperma* spp. are thought to be noncupulate ovules, whereas *Eurystoma* and *Stamnostoma* are cupulate ovules (Fig. 1, F and H). Models were placed in a wind tunnel (*4*) and helium-filled neutrally buoyant bubbles of controlled size were used to visualize complex airflow patterns around them. Mechanical similarity between the model and the fossil was assured by using appropriate Reynold's numbers (*5*). Collision of windborne pollen models (pseudopollen) was assessed by determining the aerodynamic equivalent properties of water-filled paraffin spheres and scattering these "pseudopollen" upwind of the model which was placed in various orientations to airflow (parallel, tangential, and at an angle to the direction of flow). The frequency of impact was scored and compensated for by means of relative model size to ovule dimension ratios (Table 1). The characteristic flow patterns of the models are shown in Fig. 1, A to K. Individual photographs provide only instantaneous events; therefore, composite drawings of videotape analyses are given for each model. Transitions between laminar and turbulent airflow over the models are defined by the critical Reynold's number and the geometry of the model surfaces. Maximum impact of pseudopollen on the model is seen in regions of high airflow disturbance (Table 1 and Fig. 1, A to K). In general, the progressive acropetal fusion and length reduction of the preintegumentary lobes (PL) around the nucellar apex results in the localization of laminar vortices and turbulent flow around the salpinx. Models of *G. kidstoni* oriented either parallel or tangential to the direction of airflow show laminar flow around the base of the model (fused portions of the PL) and vortices or eddies along the unfused portions of the PL. In tangential orientation, maximum eddies occur just downstream of the salpinx (Fig. 1, A and B). With higher airflow rates (Re > 80), backswelling around the megasporangium occurs. The maximum frequency of pseudopollen impact occurs in parallel orientation; pseudopollen accumulates on the adaxial surface of each PL and around the salpinx. Models of *G. latens* possessing further fusion-reduction of the PL have convergent laminar flow at the distal portion of each PL and turbulent eddies about three-fourths of the way along the ovule's length (Fig. 1, C and D). This point of turbulence coincides roughly with the position of the salpinx (Fig. 1D). Airflow is frequently seen to pass along the spaces between the unfused PL and into the dead airflow space of the nucellar apex. Maximum impact scores for pseudopollen occur toward the distal portions of each PL in parallel orientation to airflow, and on the leeward side of each PL in tangential orientation. The steamlining of *G. latens* provides for a greater localization of pollen aroung the salpinx than that observed for the less reduced ovule of *G. kidstoni* (Table 1). Ovulate cupules of *E. angulare* (Fig. 1, E and F) show pronounced fusion of the PL, resulting in a four-ridged structure with an equal number of highly reduced distal lobes around the salpinx (Fig. 1, I and J). In tangential orientation a series of regular wakes or eddies develop just behind the salpinx region. Each ridge acts as a cutting surface to airflow, while each distal lobe deflects flow acropetally both on the windward and leeward sides (Fig. 1, I and J). Extreme streamlining, except for the lobes around the salpinx, directs airflow toward the nucellar apex. Pollen impacts for *E. angulare* are high and occur mostly around the distal lobes and within the salpinx (Table 1). Ovulate cupules of *Stamnostoma huttonense* (Fig. 1, G and H) show patterns similar to those of *E. angulare*, but are more streamlined and show a higher number of pseudopollen impacts (Fig. 1K and Table 1).

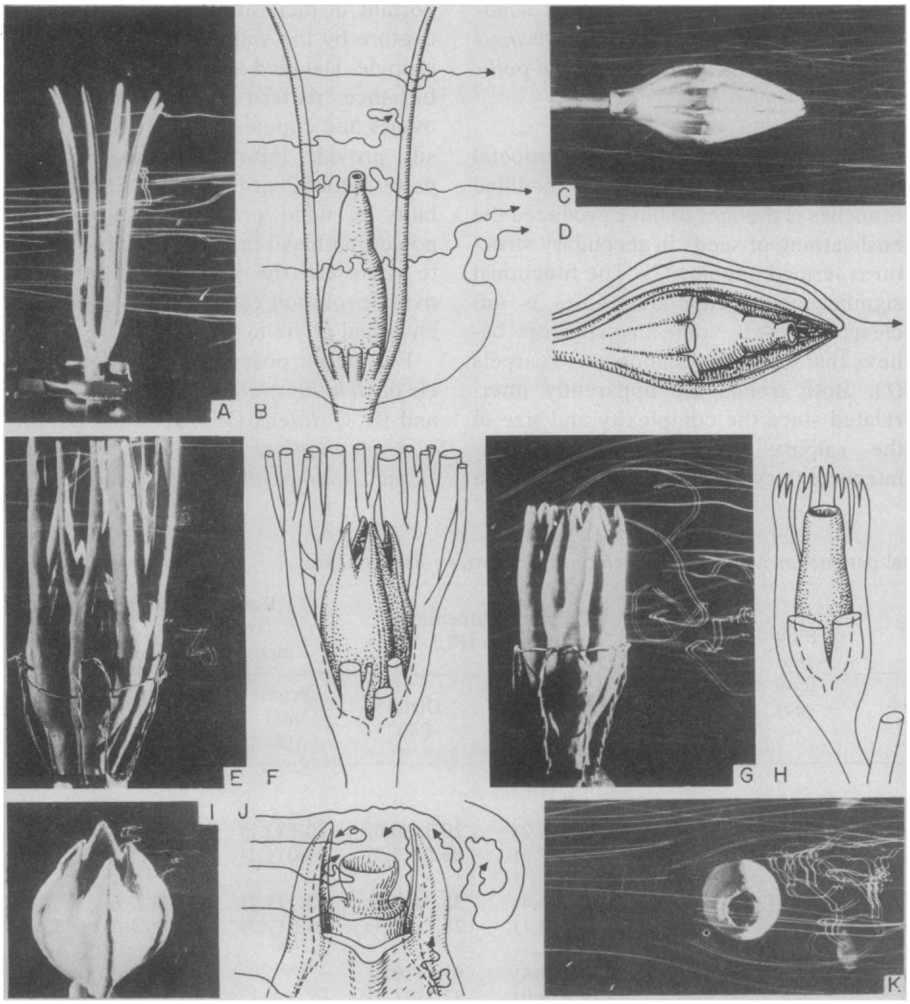

Fig. 1. Airflow patterns characteristic of representative ovule (A to D) and cupulate ovule (E to K) models in wind tunnel analyses. Flow is visualized by means of helium-filled bubbles, which when illuminated and caused to move, appear as white streaks (flow in all photographs is from left to right). (A) *Genomosperma kidstoni* in tangential orientation showing turbulent flow on the leeward side of the preintegumentary lobes (PL). (B) Composite drawing of videotape analyses of air turbulence around the nucellus of *Genomosperma kidstoni*. Each PL appears to deflect flow both upwind and downwind of the nucellus. (C) *Genomosperma latens* in parallel orientation showing laminar flow over the proximally fused PL. (D) Composite drawing of *G. latens* showing the deflection of air currents through spaces created by unfused PL toward the salpinx. (E and F) Cupulate ovule of *Eurystoma angulare* [the reconstruction is shown in (F)]. Cupule axes behave aerodynamically in much the same way as PL; turbulence occurs on the leeward side of each axis. (G and H) Cupulate ovule of *Stamnostoma huttonense* [reconstruction shown in (H)] showing cascading leeward turbulence. (I and J) Ovule of *Eurystoma angulare* showing the influence of the four distal PL over airflow. Each PL deflects flow on both the upwind and leeward surfaces (J). (K) Ovule of *Stamnostoma huttonense* in tangential flow showing leeward vortices.

The effect of the progressive consolidation of sterile lobes around the salpinx on windborne pollination may be likened to a snow fence. Particulate matter carried by the airflow is discharged on the downwind surfaces as a result of a sharp drop in airflow rate. As the PL become reduced in length and fuse acropetally, they produce a "snow fence" around the salpinx. On the basis of the data accrued by wind tunnel analyses, the localization of the snow fence increases the probability of pollination, suggesting that high efficiency in trapping pollen was a strong selective pressure involved in the evolution of the early seed plants. The data from models of *Stamnostoma* and *Eurystoma* are consistent with the snow fence scenario. As cupule axes become reduced in length and fuse acropetally, the number of pseudopollen impacting with cupule-ovule surfaces increases.

Isolated ovules of *Eurystoma* (Fig. 1I) are more efficient in trapping pollen than are cupulate ovules (Table 1). Statistically, a greater number of direct impacts occur, and a higher percentage of these reach the salpinx. Cupules of *Stamnostoma* have much the same effect and reduce the number of pseudopollen to ovule surface impacts, but they do not statistically reduce the percentage of pseudopollen which reaches the salpinx (Table 1).

The "snow fence" scenario is, however, an oversimplification. Analyses of hirsute ovules (*Salpingostoma* and *Physostoma*) indicate that the potential benefits of streamlining are mitigated by the presence of hair-bearing surfaces. Similarly, cupule axes appear to interfere with the full hypothetical potential for pollination. These data may indicate that additional selective pressures other than pollination efficiency have dictated ovule and cupule streamlining. The aerodynamic trend of ovule streamlining may have been influenced by other selective pressures such as predation. Adduction and fusion of lobes around the nucellus, the production of surface hairs, and the consolidation of many ovules into a cupule, may have served both to protect the seed or seeds or aid in their dispersal (or both). The above analyses indicate, however, that at least one significant consequence of ovule streamlining, whether through direct or indirect selective pressure, was to increase the probability of directing windborne pollen toward the salpinx and later toward the micropyle.

KARL J. NIKLAS
Division of Biological Sciences, Cornell University, Ithaca, New York 14853

References and Notes

1. H. N. Andrews, *Science* **142**, 925 (1963); A. G. Long, *Trans. R. Soc. Edinburgh* **66**, 345 (1966).
2. K. J. Niklas, B. H. Tiffney, A. H. Knoll, in *Evolutionary Biology*, M. K. Hecht, W. C. Steere, B. Wallace, Eds. (Plenum, New York, 1980), vol. 12, pp. 1-89.
3. N. E. Hughes and J. Smart, in *The Fossil Record*, W. B. Harland *et al.*, Eds. (Geological Society of London, London, 1967), pp. 107-117.
4. Flow visualization is effected by an SAI bubble generator (Sage Action, Inc., P.O. Box 416, Ithaca, N.Y. 14850) which generates neutrally buoyant helium-filled bubbles. Models are painted with a low-reflectivity paint and photographed with Tri-X Pan (ASA 400) film.
5. Airflow analogy between the model and size of ovule (Table 1) requires that the ratio of inertial and frictional forces (Reynold's number) is constant for each, such that, $Re = Vd/\nu$, Values necessary to compute Reynold's numbers are given in Table 1.
6. I thank B. Bernstein for constructing ovule and cupule models as well as illustrating flow patterns, and B. Colthart for photographic assistance. The assistance of Sage Action personnel is also gratefully acknowledged. Supported by NSF grant DEB 78-22646.

15 May 1980; revised 23 July 1980

A Scanning Micropipette Molecule Microscope

Abstract. *A movable quartz micropipette, whose tip is sealed with a polymer plug, is used as a liquid-vacuum interface to a mass spectrometer. A light microscope allows observation of, and positioning of, the micropipette tip on the surface of a sample mounted in a perfusion chamber. This forms the basis of an instrument which enables one to study, in vitro, the localization of transepithelial transport of water and other molecules. Some preliminary results from the use of this instrument are presented.*

The in vitro localization of the pathways of water transport is a problem of general interest in epithelial physiology. We have developed an instrument which provides a direct, real-time measure of water transport, with a spatial resolution of 2 to 5 μm, across a living epithelium.

A simplified diagram is shown in Fig. 1a. The instrument consists of a perfusion chamber that will allow simultaneous observation of a sample and the tip, 1 to 10 μm in diameter, of a quartz micropipette. The tip of the micropipette is sealed with a small plug of a permeable material such as dimethyl siloxane-polycarbonate copolymer or cellulose acetate (Fig. 1b) (*1*). The shank of the micropipette is connected by means of a flexible vacuum coupling to the inlet of the ionizer of a quadrupole mass spectrometer and is hence under vacuum. The micropipette is inserted in solution and scanned over (or placed at various points on) the surface of the sample, much as in the microelectrode experiments of Frömter and Diamond (*2*). Molecules that permeate the plug in sufficient amount can be detected by the quad-

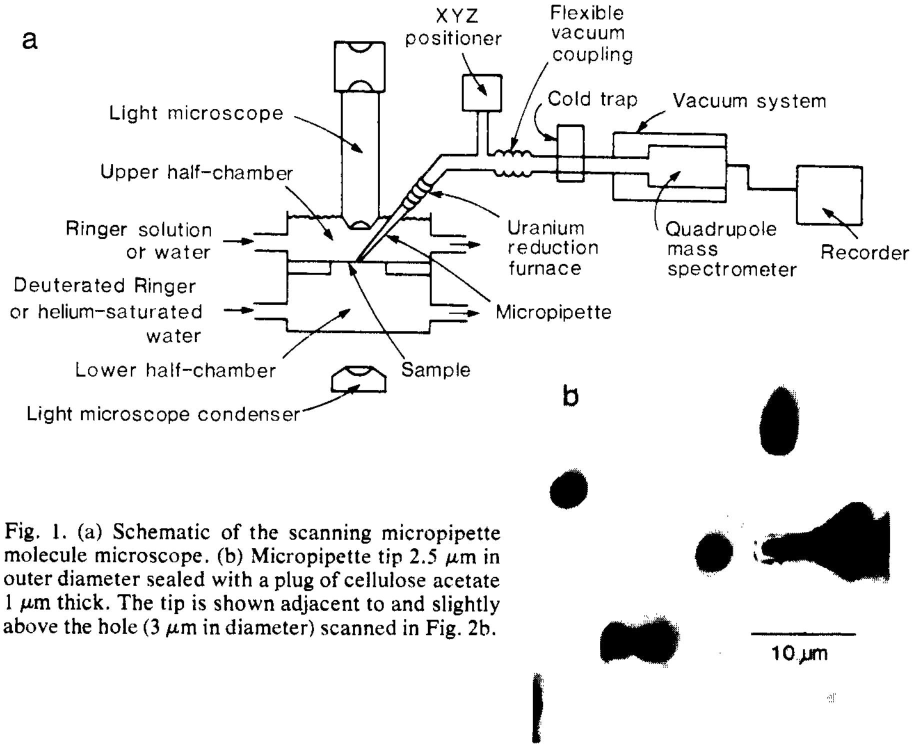

Fig. 1. (a) Schematic of the scanning micropipette molecule microscope. (b) Micropipette tip 2.5 μm in outer diameter sealed with a plug of cellulose acetate 1 μm thick. The tip is shown adjacent to and slightly above the hole (3 μm in diameter) scanned in Fig. 2b.

0036-8075/81/0116-0277$00.50/0 Copyright © 1981 AAAS